



---

# **Studies of Inviscid Flux Schemes for Acoustics and Turbulence Problems**

**Chris Morris**

**NASA Marshall Space Flight Center**

**Aerosciences Branch/EV33**

**January 7, 2013**



# Objectives

---

- ◆ **Determine the suitability of various inviscid flux schemes for:**
  - Acoustics problems
  - Directly resolving turbulence
  - Large-eddy simulations of turbulence
  
- ◆ **Provide guidance for the long-term evolution of our Loci-based CFD codes**
  - Focus is on the compressible Navier-Stokes equations due to wide range of applicability
  - Emphasis in this paper is on the basic resolving characteristics of spatial discretizations and inviscid fluxes, not on LES sub-grid scale (SGS) models
  - Grid resolutions considered here are from DNS levels to fine-grid LES levels



**DNS**

# **Turbulence Modeling Strategies**

---

**Directly resolve all scales of turbulent motion. There is no eddy viscosity, and the intrinsic dissipation of the inviscid flux must be  $\ll$  laminar viscosity.**

**LES/ILES**

**Directly resolve largest scales of turbulent motion, and model the smaller scales using one of two approaches: A) classic LES - a subgrid-scale (SGS) turbulence model, requiring that the intrinsic dissipation of the inviscid flux is  $\ll$  SGS eddy viscosity, or B) ILES – where the intrinsic dissipation of a 2<sup>nd</sup> order accurate inviscid flux approximately mimics the SGS eddy viscosity.**

**HRANS-LES**

**Attempts to directly resolve turbulence only in regions with adequate grid resolution, otherwise turbulence is modeled. In LES regions the algorithmic requirements would be consistent with the above description.**

**RANS**

**Turbulence is entirely modeled.**



# Governing Equations of Fluid Mechanics

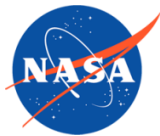
## Navier-Stokes Equations in Terms of Conservative Variables:

$$\frac{d\mathbf{U}}{dt} + \frac{d(\mathbf{F}_i - \mathbf{F}_v)}{dx} + \frac{d(\mathbf{G}_i - \mathbf{G}_v)}{dy} + \frac{d(\mathbf{H}_i - \mathbf{H}_v)}{dz} = \mathbf{W}$$

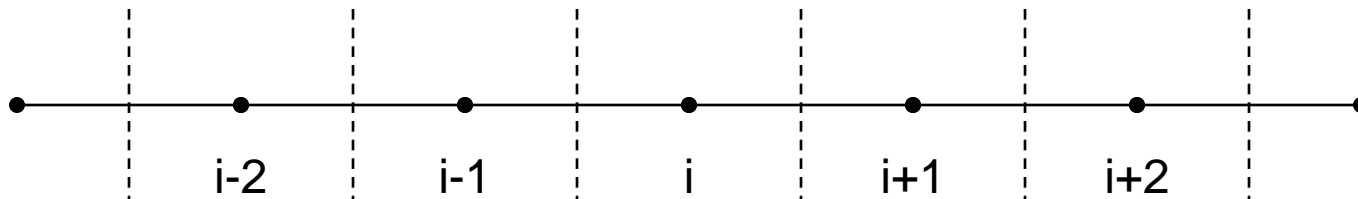
$$\mathbf{U} = \begin{Bmatrix} \rho \\ \rho u \\ \rho v \\ \rho w \\ \rho E_{\text{tot}} \end{Bmatrix} \quad \mathbf{F}_i = \begin{Bmatrix} \rho u \\ \rho u^2 + P \\ \rho uv \\ \rho uw \\ \rho u H_{\text{tot}} \end{Bmatrix} \quad \mathbf{F}_v = \begin{Bmatrix} 0 \\ \tau_{xx} \\ \tau_{xy} \\ \tau_{xz} \\ u\tau_{xx} + v\tau_{xy} + w\tau_{xz} - q_x \end{Bmatrix} \quad \text{Etc.}$$

## Conservative Differencing Forms the Flux at a Half-Point:

$$\frac{d\mathbf{U}}{dt} + \frac{d\mathbf{F}(\mathbf{U})}{dx} = 0 \quad \Rightarrow \quad \frac{d\mathbf{U}}{dt} = -\frac{d\mathbf{F}(\mathbf{U})}{dx} \quad \Rightarrow \quad \Delta \mathbf{U}_i = -(\Delta t / \Delta x)(\mathbf{F}_{i+1/2} - \mathbf{F}_{i-1/2})$$



# Central Difference Schemes



CD-2  $\mathbf{F}_{i+1/2} = \mathbf{F}_{\text{avg}}(i, i+1)$

CD-4  $\mathbf{F}_{i+1/2} = (4/3)\mathbf{F}_{\text{avg}}(i, i+1) - (1/6)[\mathbf{F}_{\text{avg}}(i-1, i+1) + \mathbf{F}_{\text{avg}}(i, i+2)]$

CD-6  $\mathbf{F}_{i+1/2} = (3/2)\mathbf{F}_{\text{avg}}(i, i+1) - (3/10)[\mathbf{F}_{\text{avg}}(i-1, i+1) + \mathbf{F}_{\text{avg}}(i, i+2)]$   
 $+ (1/30)[\mathbf{F}_{\text{avg}}(i-2, i+1) + \mathbf{F}_{\text{avg}}(i-1, i+2) + \mathbf{F}_{\text{avg}}(i, i+3)]$

CD-8  $\mathbf{F}_{i+1/2} = (16/10)\mathbf{F}_{\text{avg}}(i, i+1) - (4/10)[\mathbf{F}_{\text{avg}}(i-1, i+1) + \mathbf{F}_{\text{avg}}(i, i+2)]$   
 $+ (8/105)[\mathbf{F}_{\text{avg}}(i-2, i+1) + \mathbf{F}_{\text{avg}}(i-1, i+2) + \mathbf{F}_{\text{avg}}(i, i+3)]$   
 $- (1/140)[\mathbf{F}_{\text{avg}}(i-3, i+1) + \mathbf{F}_{\text{avg}}(i-2, i+2) + \mathbf{F}_{\text{avg}}(i-1, i+3) + \mathbf{F}_{\text{avg}}(i, i+4)]$

CF-2  $\mathbf{F}_{i+1/2} = (3/2)\mathbf{F}_{\text{avg}}(i, i+1) - (1/4)[\mathbf{F}_{\text{avg}}(i-1, i+1) + \mathbf{F}_{\text{avg}}(i, i+2)]$

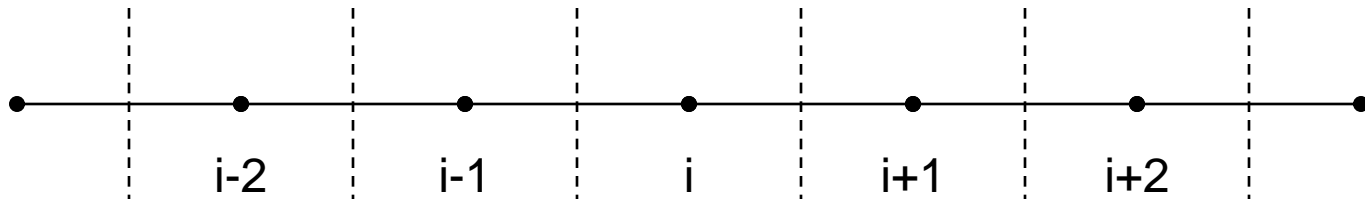
$$\mathbf{F}_{\text{avg}}(i_1, i_2) = \frac{1}{2}(\rho_{i_1} + \rho_{i_2}) \frac{1}{2}(u_{i_1} + u_{i_2}) \frac{1}{2}(\mathbf{V}_{i_1} + \mathbf{V}_{i_2}) + \frac{1}{2}(\mathbf{P}_{i_1} + \mathbf{P}_{i_2})$$

where  $\mathbf{V} = [1, u, v, w, H_{\text{tot}}]$  and  $\mathbf{P} = [0, P, 0, 0, 0]$

As shown by Pirozzoli (2010), this  $\mathbf{F}_{\text{avg}}$  reproduces the skew-symmetric scheme of Kennedy and Gruber (2008). Note if  $\mathbf{F}_{\text{avg}} = (\mathbf{F}_{i_1} + \mathbf{F}_{i_2})$ , then standard divergence form central differencing formulas result.



# Upwind Schemes



**Roe Flux using “left” and “right” interpolations for the half-node**

$$\mathbf{F}_{i+1/2} = \frac{1}{2}(\mathbf{F}_{i+1/2,L} + \mathbf{F}_{i+1/2,R}) - \frac{1}{2}|\mathbf{A}_{\text{roe}}|(\mathbf{U}_{i+1/2,R} - \mathbf{U}_{i+1/2,L})$$

where  $\mathbf{F}_{i+1/2,L}$  and  $\mathbf{U}_{i+1/2,L}$  are formed from  $[\rho, u, v, w, P]_{i+1/2,L}$   
 and  $\mathbf{F}_{i+1/2,R}$  and  $\mathbf{U}_{i+1/2,R}$  are formed from  $[\rho, u, v, w, P]_{i+1/2,R}$

**Primitive variable reconstruction for generic flow variable  $\phi$  (no slope limiting)**

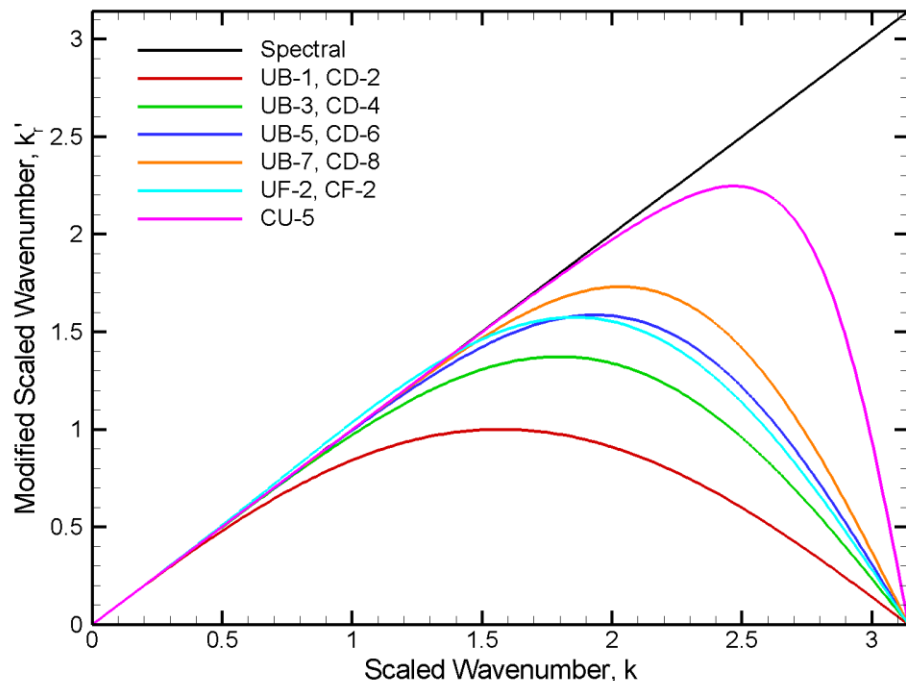
UB-1	$\phi_{i+1/2,L} = \phi_i$
UB-3	$\phi_{i+1/2,L} = (-\phi_{i-1} + 5\phi_i + 2\phi_{i+1})/6$
UB-5	$\phi_{i+1/2,L} = (4\phi_{i-2} - 26\phi_{i-1} + 94\phi_i + 54\phi_{i+1} - 6\phi_{i+2})/120$
UB-7	$\phi_{i+1/2,L} = (-6\phi_{i-3} + 50\phi_{i-2} - 202\phi_{i-1} + 638\phi_i + 428\phi_{i+1} - 76\phi_{i+2} + 8\phi_{i+3})/840$
UF-2	$\phi_{i+1/2,L} = (-\phi_{i-1} + 4\phi_i + \phi_{i+1})/4$
CU-5	$3\phi_{i-1/2,L} + 6\phi_{i+1/2,L} + \phi_{i+3/2,L} = (\phi_{i-1} + 19\phi_i + 10\phi_{i+1})/3$

The  $\phi_{i+1/2,R}$  values are formed from a flipped interpolation

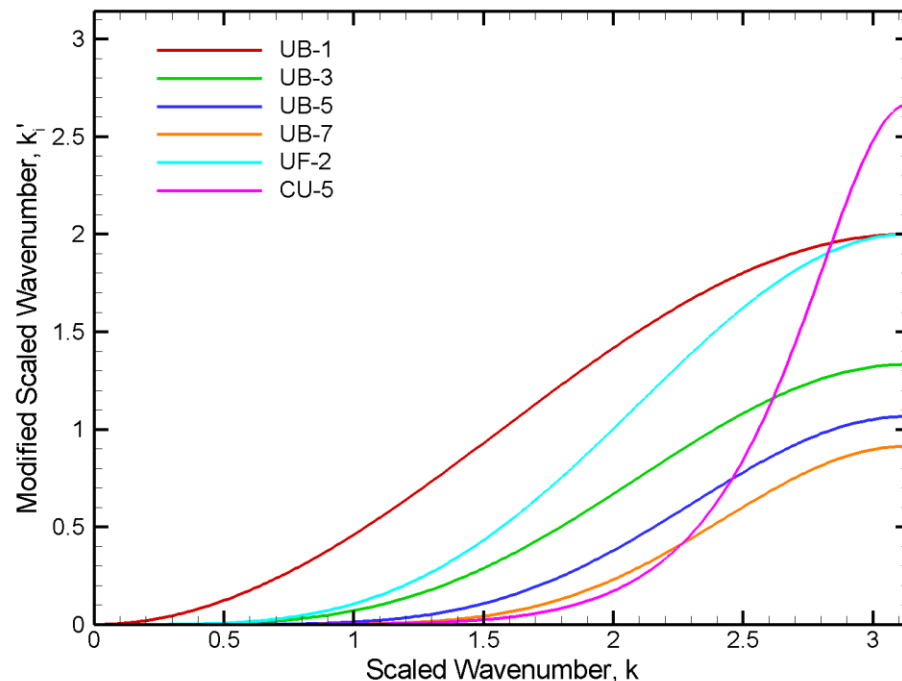


# Fourier Analysis Characteristics

Real Part of Modified Scaled Wave-number: Dispersion (Phase)



Imaginary Part of Modified Scaled Wave-number: Dissipation



- ◆ The dispersion (phase) characteristics of each UB scheme are the same as the CD scheme of one higher order of accuracy
- ◆ UB-1 and CD-2 have a limited range of phase accuracy, while CU-5 has a relatively wide range
- ◆ Central schemes are non-dissipative, while all upwind schemes experience increasing dissipation error at higher wavenumbers
- ◆ Higher-order upwind schemes have smaller dissipation error at lower wavenumbers than lower-order upwind schemes



# 1-D Acoustic Standing Wave Problem

---

Air at  $P_0 = 101325$  Pa,  $T_0 = 25$  °C,  $R = 287$  J/Kg-K,  $\rho_0 = 1.18413$  kg/m<sup>3</sup>,  
 $a_0 = 346.117$  m/s

$u(x,t=0) = U_0 \cos(nx/l)$ , where  $0 \leq x \leq 2\pi l$ ,  $l = 1$  m,  $U_0 = 0.1$  m/s,  
and  $n$  is the desired initial number of wavelengths

Grid: 128 grid points, uniform spacing, periodic B.C.

Assuming isentropic flow and small disturbances, the Euler equations can be simplified to the linearized equations of gas dynamics. The resulting exact solution is

$$U(x,t) = 0.5U_0(\cos(n(x - at)/l) + \cos(n(x + at)/l)) = U_0 \cos(nx/l) \cos(nat/l)$$

$$P(x,t) - P_0 = 0.5\rho_0 a_0 U_0 (\cos(n(x - at)/l) - \cos(n(x + at)/l)) = \\ \rho_0 a_0 U_0 \sin(nx/l) \sin(nat/l)$$

4-stage Runge-Kutta time advancement, CFL = 1.0, 0.5 or 0.25

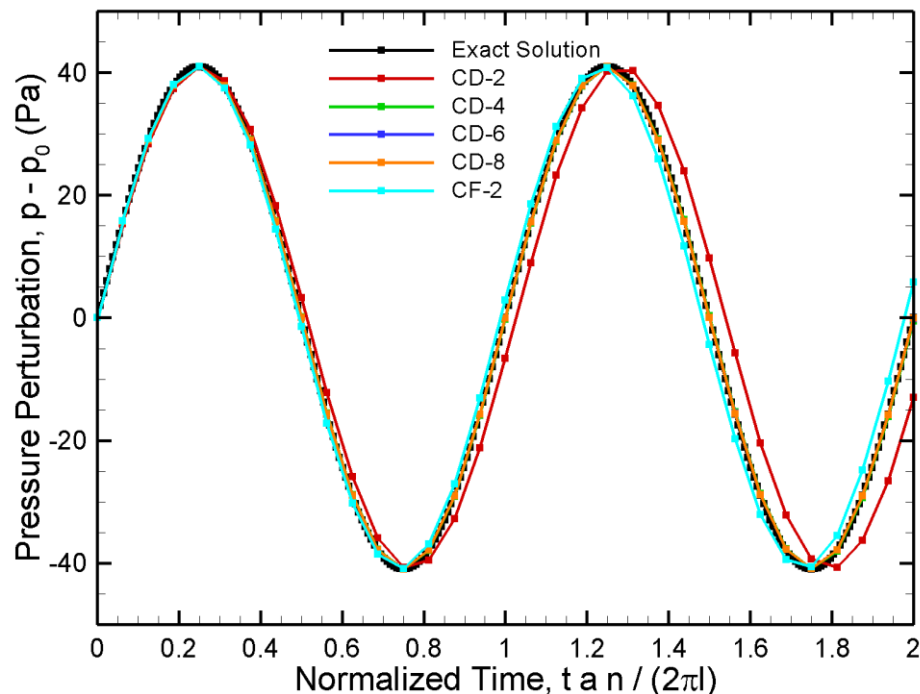




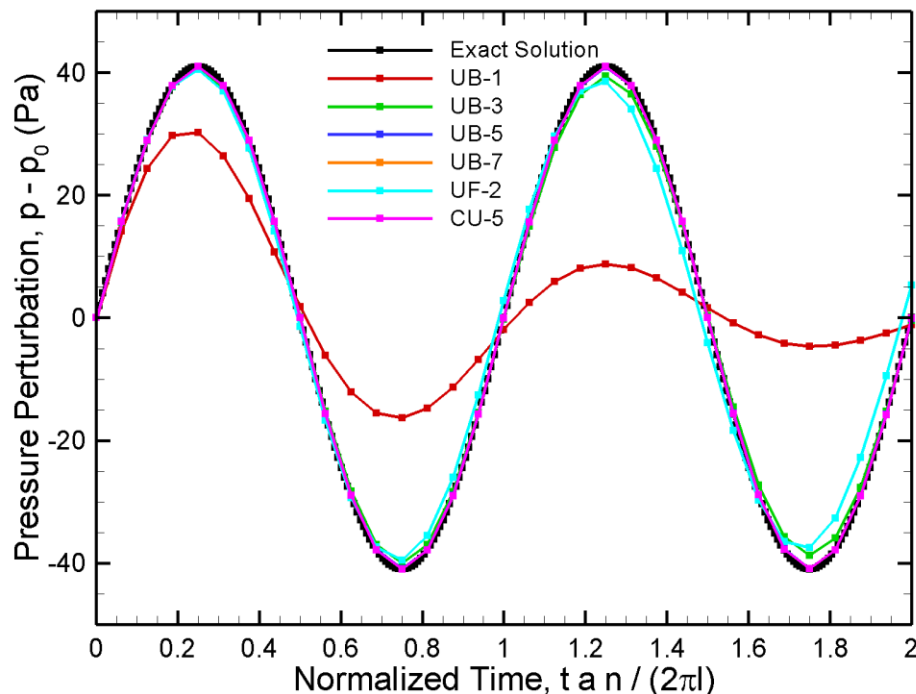
# Pressure History at First Pressure Antinode

$n = 8, 16 \text{ PPW}, k = \pi/8$

## Central Difference Schemes



## Upwind Schemes



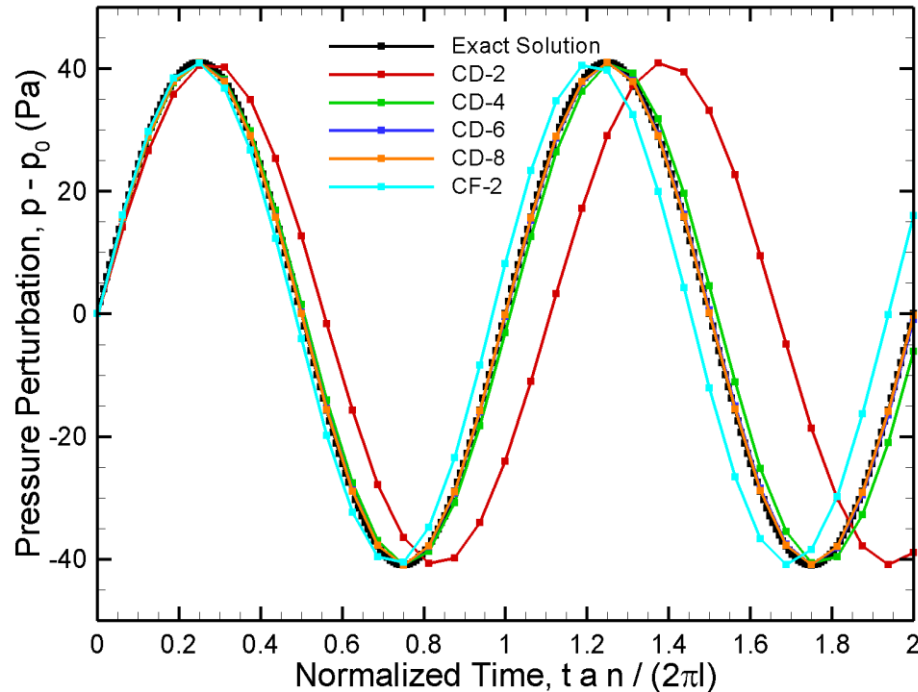
- ◆  $\Delta t = (1/16) 2\pi l / a n$ , CFL = 1.0
- ◆ Some dispersion error noticeable for CD-2 scheme
- ◆ Dissipation is already severe for UB-1, barely noticeable for UF-2 and UB-3



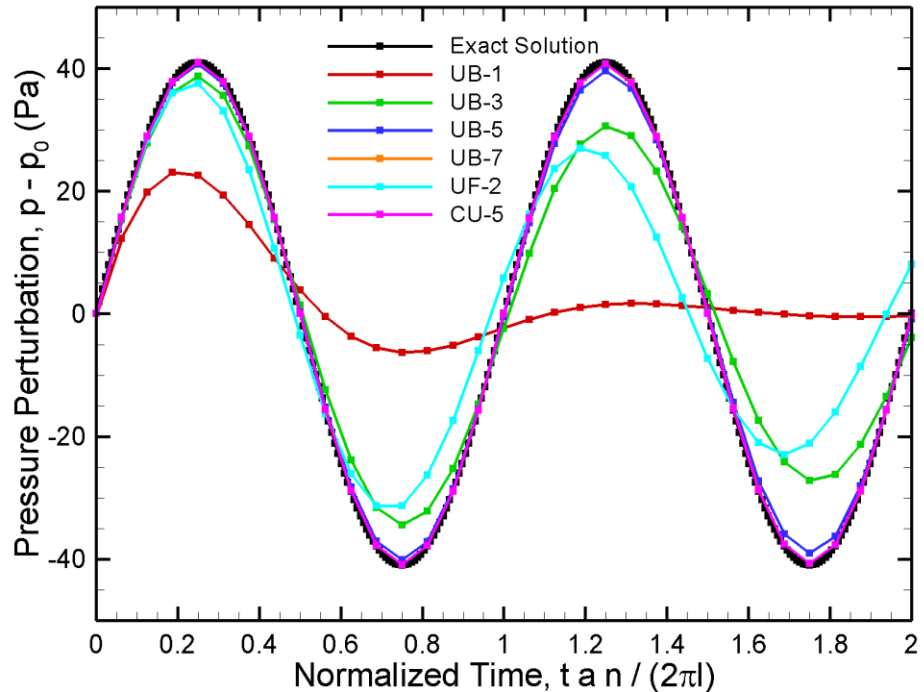
# Pressure History at First Pressure Antinode

$n = 16, 8 \text{ PPW}, k = \pi/4$

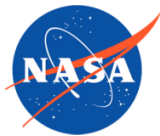
## Central Difference Schemes



## Upwind Schemes



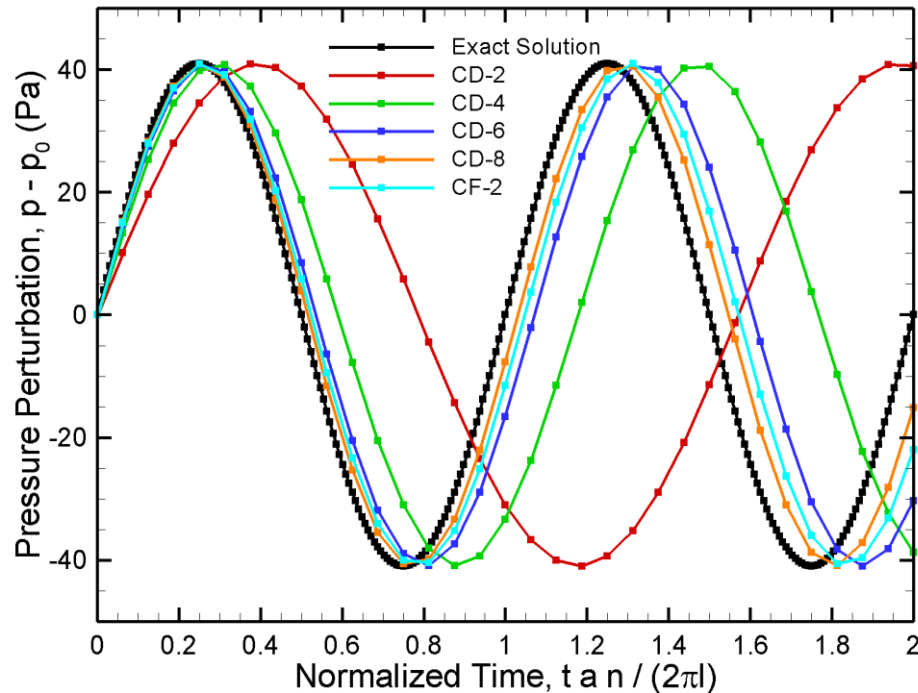
- ◆  $\Delta t = (1/16) 2\pi l / a n$ , CFL = 0.5
- ◆ Dispersion error for CD-2 scheme now more significant
- ◆ Some dispersion error for CF-2 noticeable in opposite direction
- ◆ Dissipation even worse for UB-1, and now significant for UF-2 and UB-3



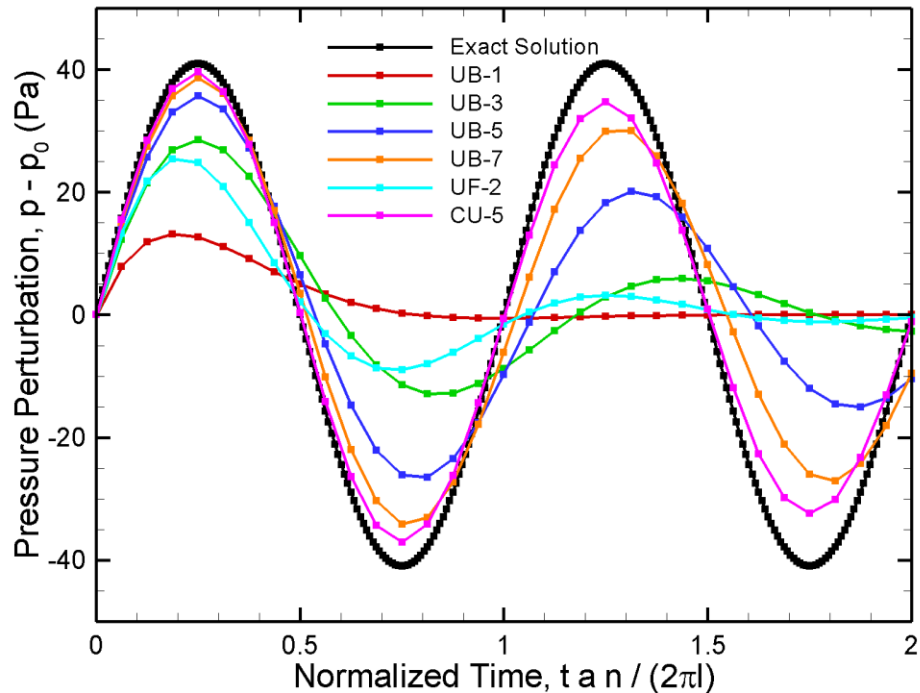
# Pressure History at First Pressure Antinode

$n = 32, 4 \text{ PPW}, k = \pi/2$

## Central Difference Schemes



## Upwind Schemes



- ◆  $\Delta t = (1/16) 2\pi l / a n$ , CFL = 0.25
- ◆ Dispersion error severe for CD-2, significant for CD-4, and noticeable for the other central schemes
- ◆ Dissipation severe for UB-1, UB-3 and UF-2, and significant for all other upwind schemes
- ◆ The least dissipative is CU-5, which also has the best dispersion accuracy



# Taylor-Green Vortex Problem

---

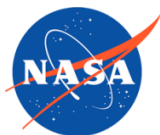
Air at  $P_0 = 7271$  Pa,  $T_0 = 25$  °C,  $R = 287$  J/Kg-K,  $\rho_0 = 0.0849723$  Kg/m<sup>3</sup>,  
 $a_0 = 346.117$  m/s,  $U_0 = 0.1 a_0 = 34.6117$  m/s,  $\mu_0 =$  Sutherland relation,  
 $Re = \rho_0 U_0 l / \mu_0 = 1600$

$$\begin{aligned}u(x,y,z,t=0) &= U_0 \sin(x/l) \cos(y/l) \cos(z/l), \\v(x,y,z,t=0) &= -U_0 \cos(x/l) \sin(y/l) \cos(z/l), \\w(x,y,z,t=0) &= 0, \\p(x,y,z,t=0) &= p_0 + (\rho_0 U_0^2 / 16) [\cos(2x/l) + \cos(2y/l)] [\cos(2z/l) + 2] \\ \rho(x,y,z,t=0) &= p / RT_0 \\ \text{where } -\pi l \leq x \leq \pi l, -\pi l \leq y \leq \pi l, -\pi l \leq z \leq \pi l, l &= 0.01 \text{ m}\end{aligned}$$

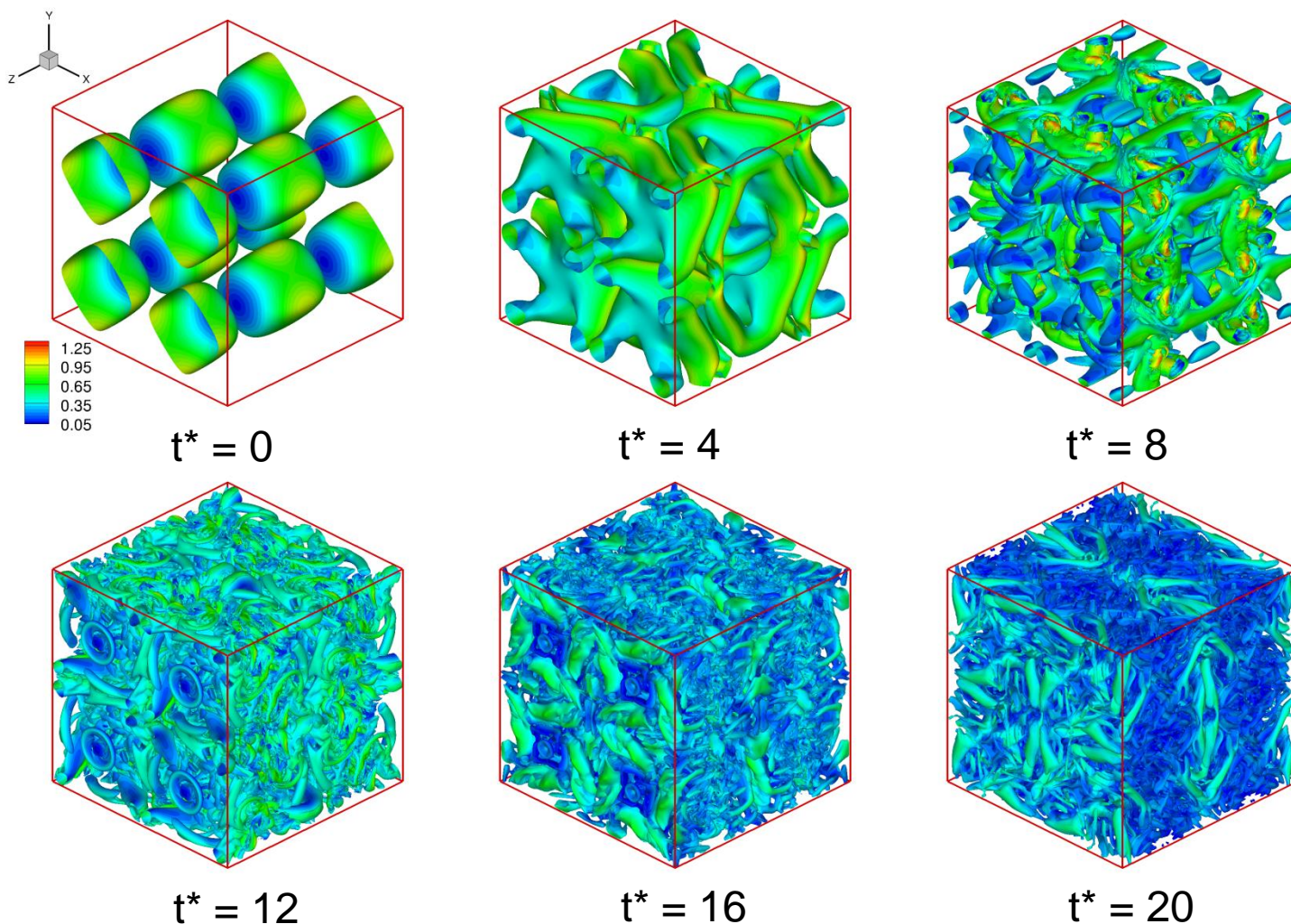
Grids:  $256 \times 256 \times 256$ ,  $192 \times 192 \times 192$  and  $128 \times 128 \times 128$  grid points,  
uniform spacing, periodic B.Cs.

4-stage Runge-Kutta time advancement,  $CFL \approx 0.45$  on  $256 \times 256 \times 256$  grid

DNS results have been calculated by Brachet et al. (1983) and van Rees et al. (2011). Also see <http://www.public.iastate.edu/zjw/hiocfd.html>.



# Iso-surfaces of Q-criterion $Q = 0.1 (U_0/l)^2$ Taylor-Green Vortex Problem at $Re = 1600$



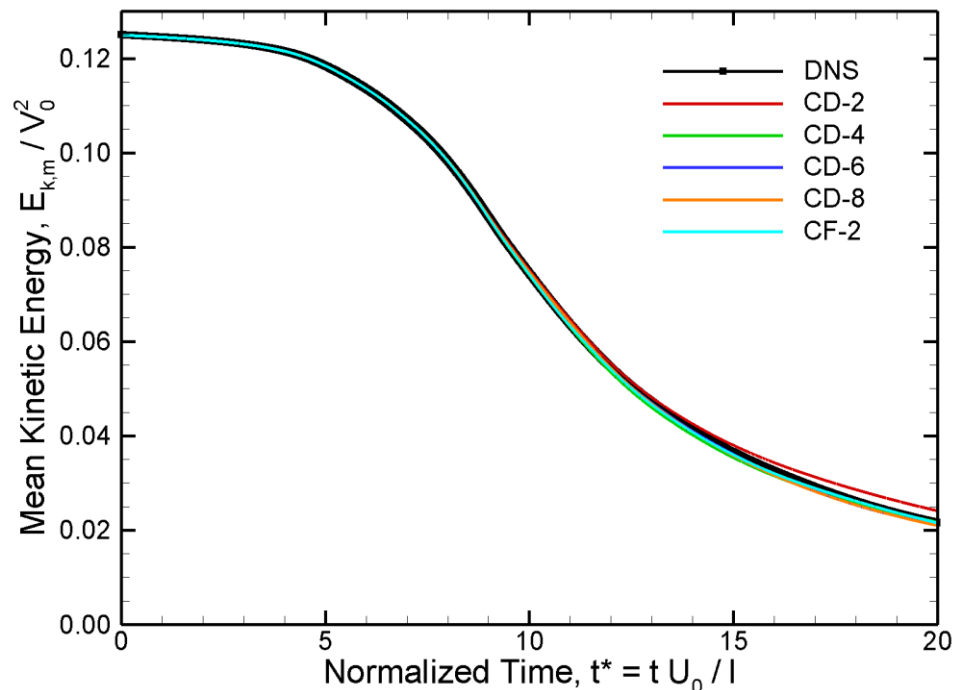
- ◆ Simulation run using CD-8 scheme on  $256 \times 256 \times 256$  point grid
- ◆ Iso-surfaces colored by velocity magnitude  $U/U_0$
- ◆  $t^*$  is a normalized timescale  $tU_0/l$



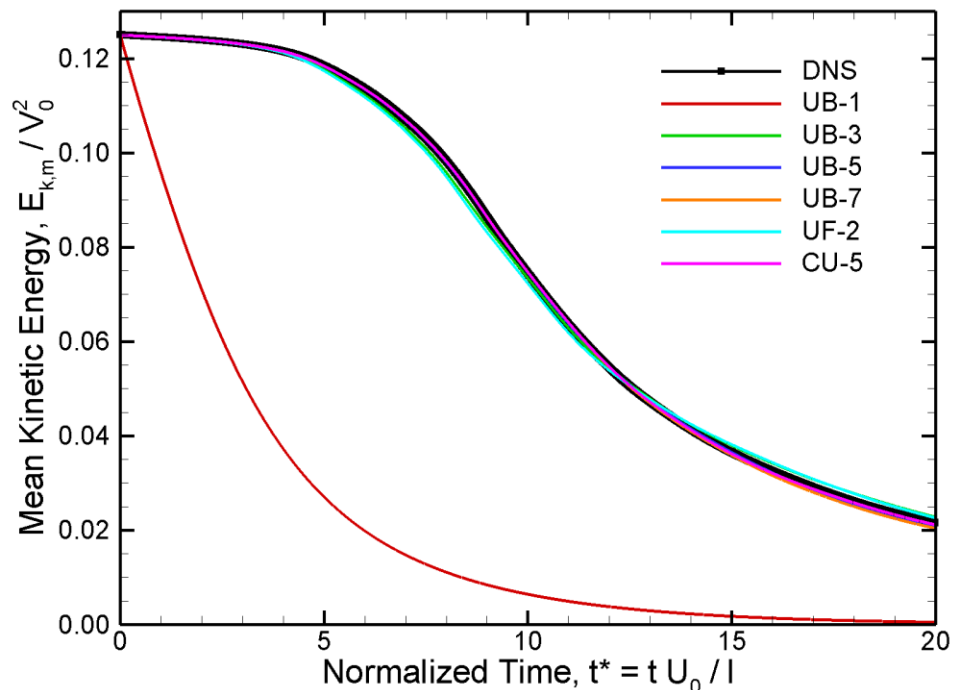
# Mean Kinetic Energy History

## 256 × 256 × 256 Point Grid

### Central Difference Schemes



### Upwind Schemes



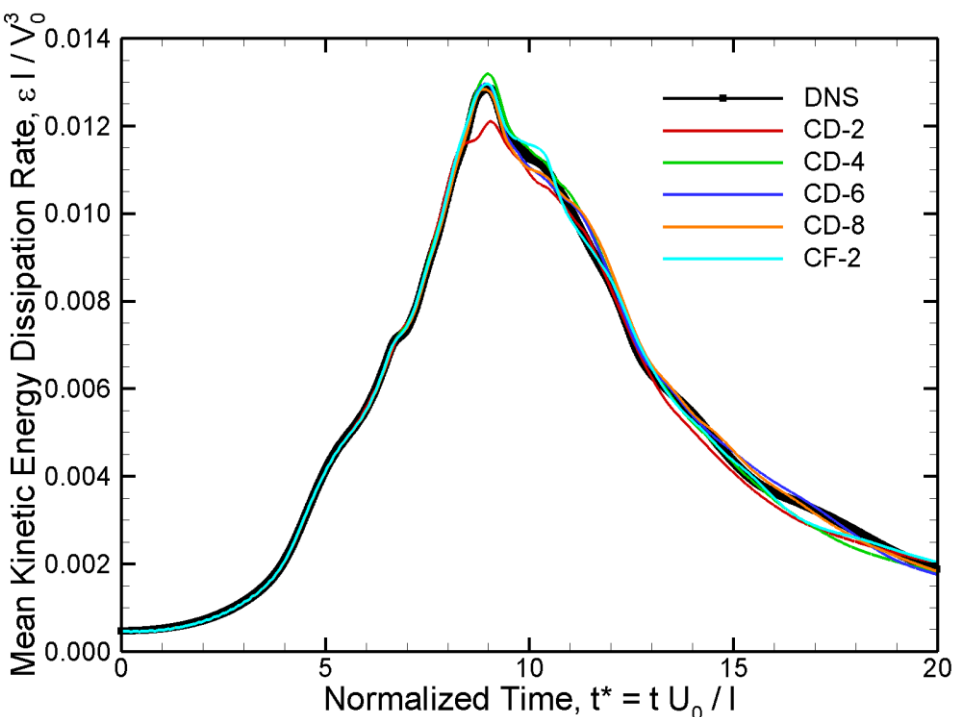
- ◆ The central schemes generally follow the DNS kinetic energy history very well, though CD-2 differs slightly toward the end
- ◆ The UB-1 scheme rapidly dissipates all kinetic energy in the flow
- ◆ UB-3 and UF-2 are much closer to the DNS, though some differences are evident.
- ◆ The remaining upwind schemes follow the DNS very closely



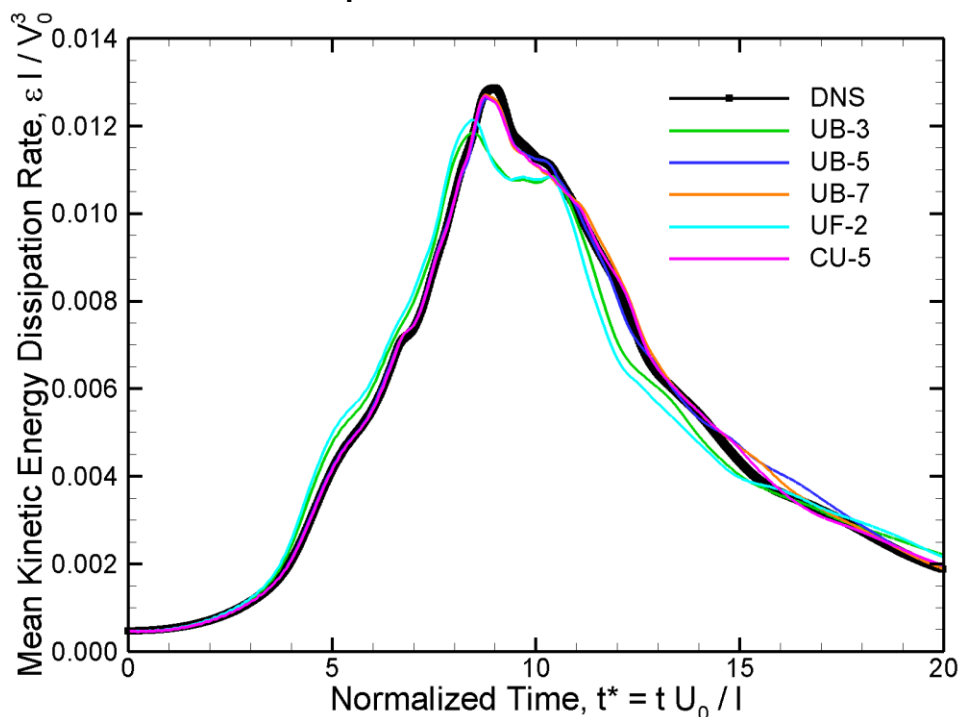


# Measured Mean Kinetic Energy Dissipation Rate History, $256 \times 256 \times 256$ Point Grid

## Central Difference Schemes



## Upwind Schemes



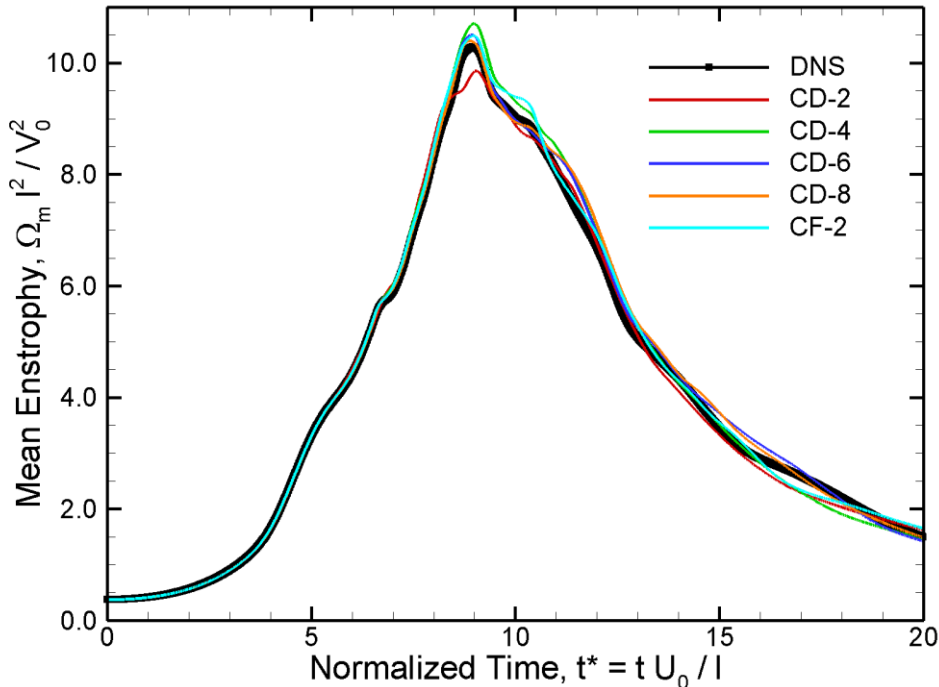
- ◆ The central schemes generally follow the DNS kinetic energy dissipation history very well, though CD-2 misses the peak at  $t^* = 9$
- ◆ The UB-1 scheme has such a high dissipation rate that it is not shown
- ◆ UB-3 and UF-2 are much closer to the DNS, though both are overly dissipative through  $t^* = 8$ , and peak earlier at a lower value
- ◆ The remaining upwind schemes follow the DNS very closely



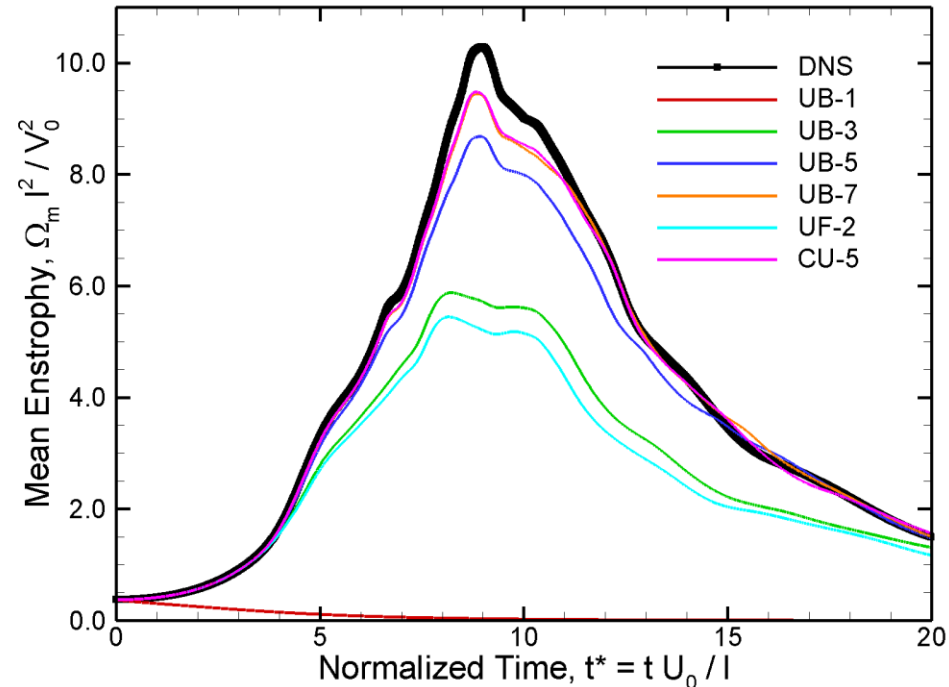
# Mean Enstrophy History

## 256 × 256 × 256 Point Grid

### Central Difference Schemes



### Upwind Schemes

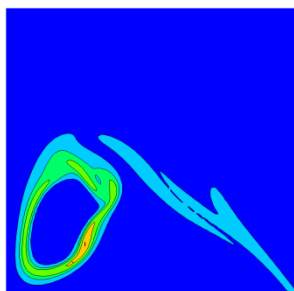


- ◆ The central schemes generally follow the DNS enstrophy history very well, though CD-2 misses the peak at  $t^* = 9$
- ◆ The UB-1 scheme rapidly dissipates all enstrophy in the flow
- ◆ The remaining upwind schemes also all fail to match the DNS, with UF-2 having the worst agreement, and CU-5 the best

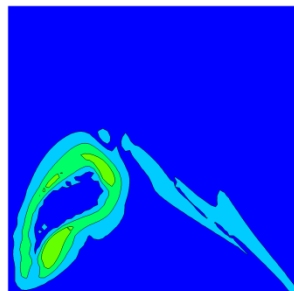




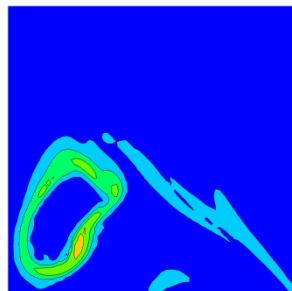
# Iso-contours of Vorticity Magnitude $|\omega|/U_0$ 256 × 256 × 256 Point Grid at $t^* = 8$



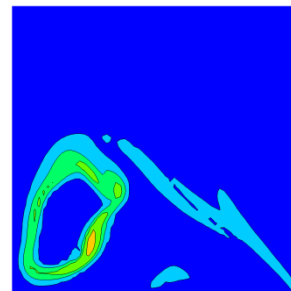
DNS



CD-2

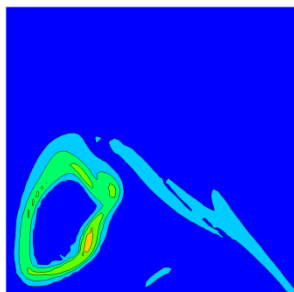


CD-4

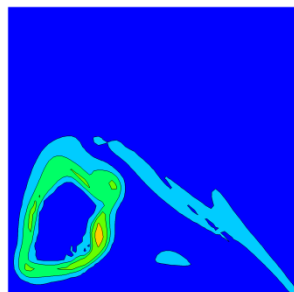


CD-6

Note: DNS was run  
on a 512 × 512 × 512  
point grid



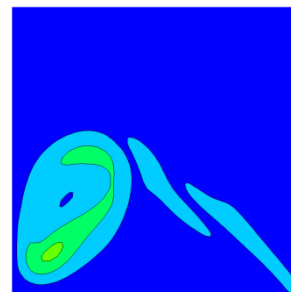
CD-8



CF-2

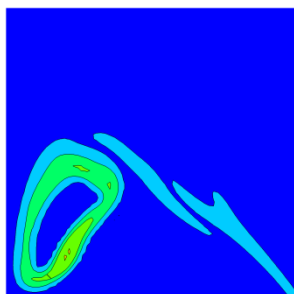


UB-1

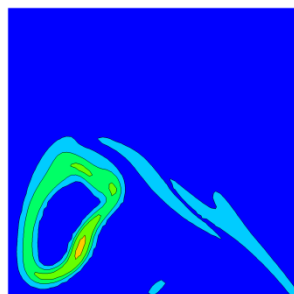


UB-3

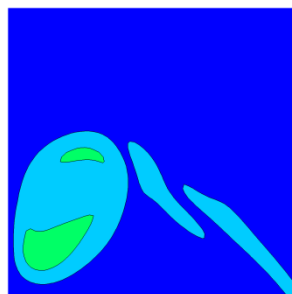
Contour Levels:  
1, 5, 10, 20 and 30



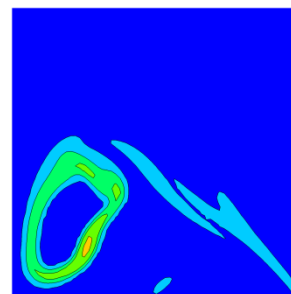
UB-5



UB-7



UF-2



CU-5

$x = 0$  plane  
 $\pi/2 \leq y \leq \pi$   
 $\pi/2 \leq z \leq \pi$

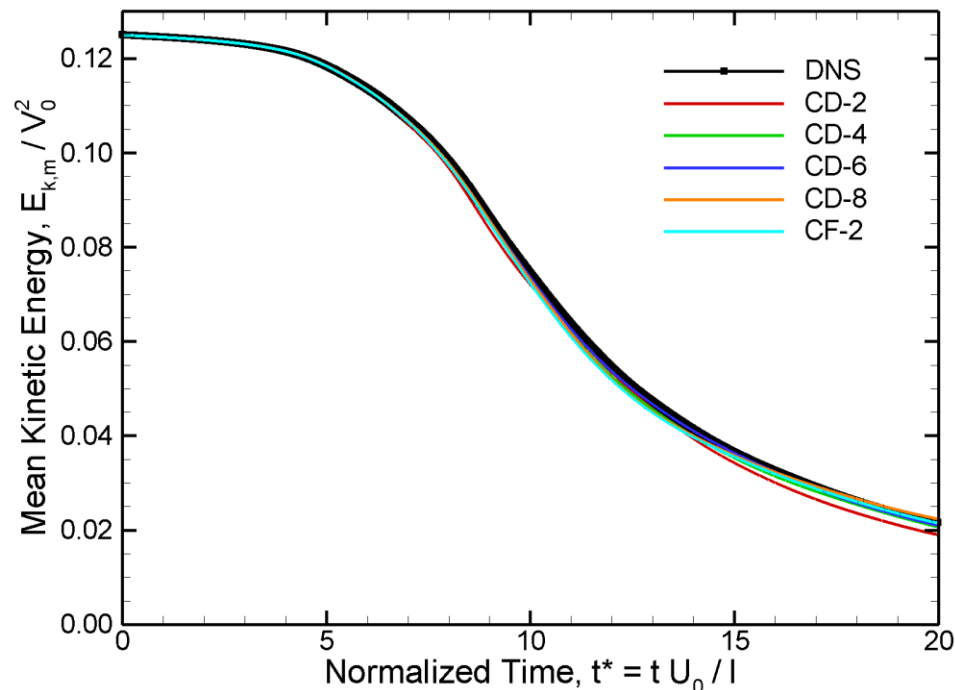
- ◆ Dissipation severe for UB-1, very noticeable for UF-2 and UB-3
- ◆ Good results for other schemes, though lack of sharpness for CD-2



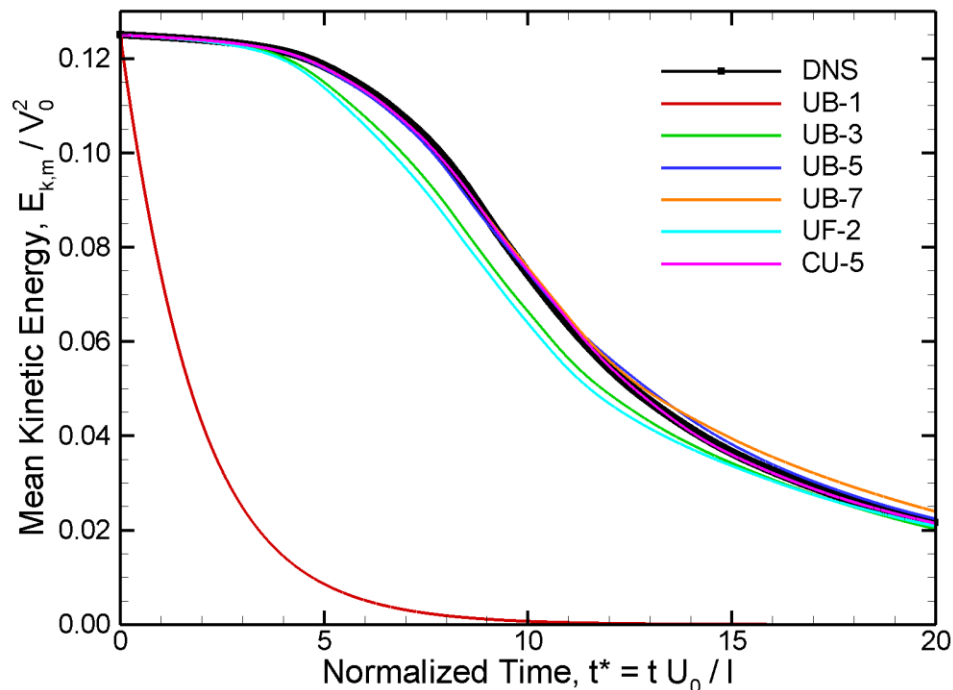
# Mean Kinetic Energy History

## 128 × 128 × 128 Point Grid

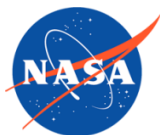
### Central Difference Schemes



### Upwind Schemes

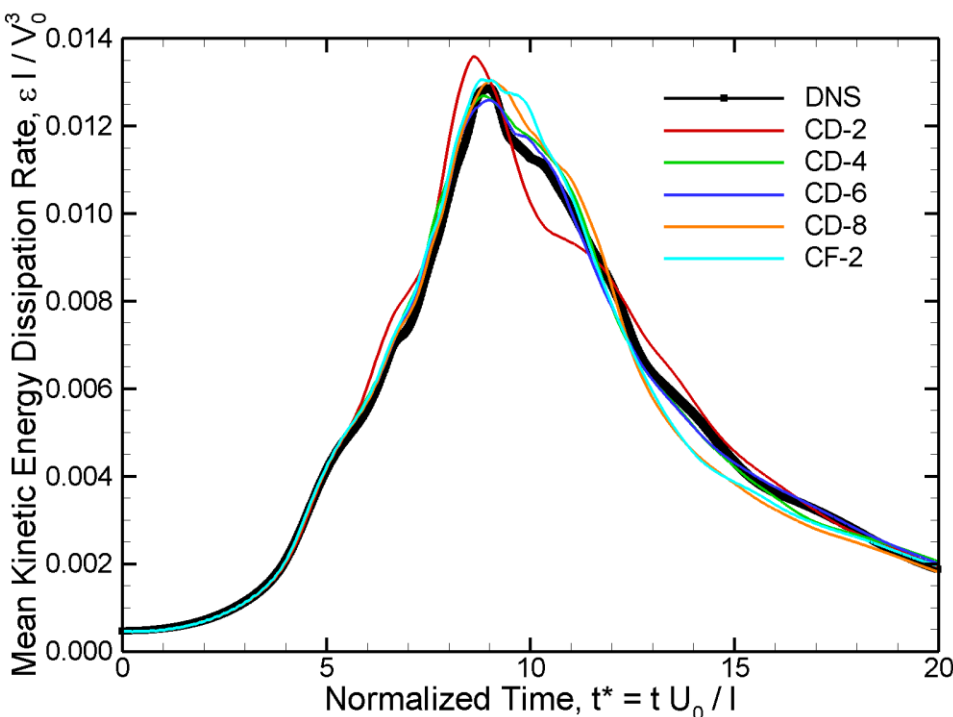


- ◆ The central schemes generally follow the DNS kinetic energy history reasonably well, though CD-2 differs slightly toward the end
- ◆ The UB-1 scheme rapidly dissipates all kinetic energy in the flow
- ◆ UB-3 and UF-2 noticeably diverge from the DNS
- ◆ UB-5, UB-7 and CU-5 follow the DNS reasonably well

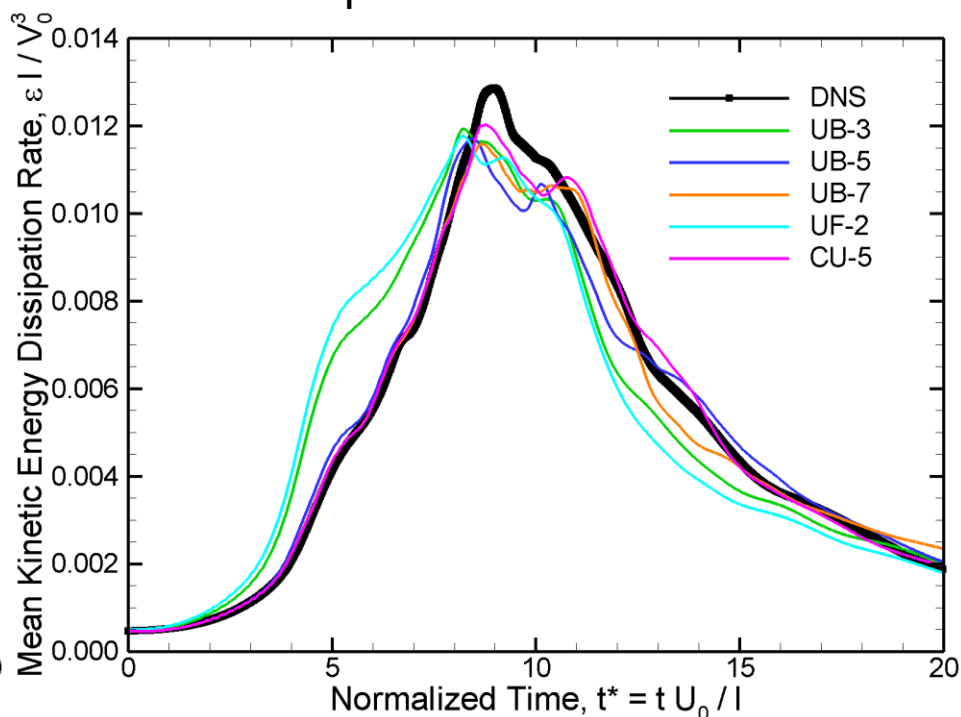


# Measured Mean Kinetic Energy Dissipation Rate History, $128 \times 128 \times 128$ Point Grid

## Central Difference Schemes



## Upwind Schemes

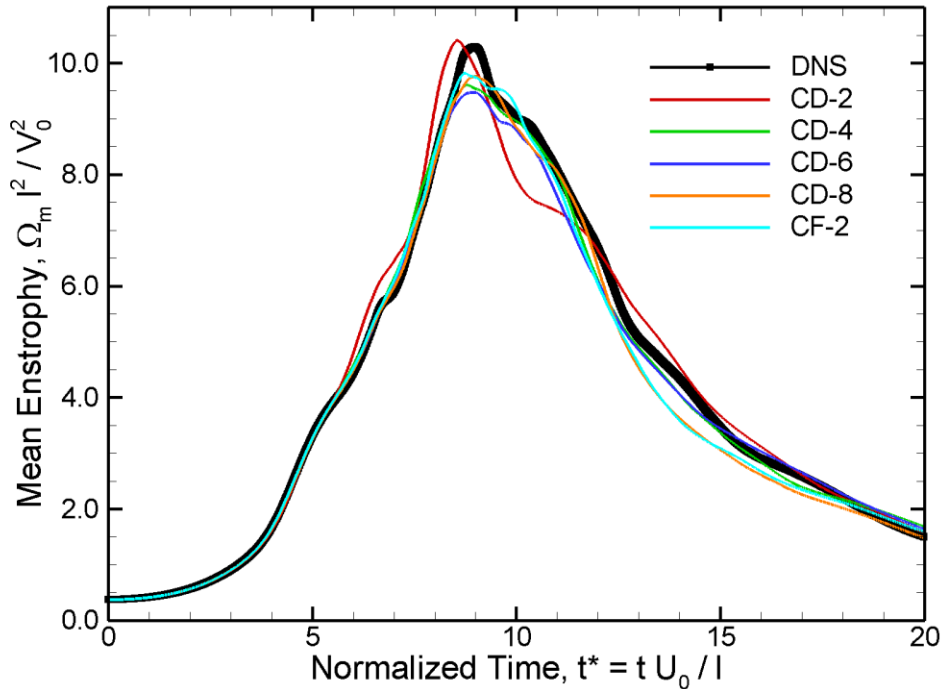


- ◆ The central schemes generally follow the DNS kinetic energy dissipation history reasonably well, though CD-2 peaks higher and earlier than the others
- ◆ The UB-1 scheme has such a high dissipation rate that it is not shown
- ◆ UB-3 and UF-2 have a significantly higher dissipation rate than the DNS for  $t^* = 0-8$ , and have a lower peak earlier in time
- ◆ UB-5, UB-7 and CU-5 do much better, but none capture the peak of the DNS

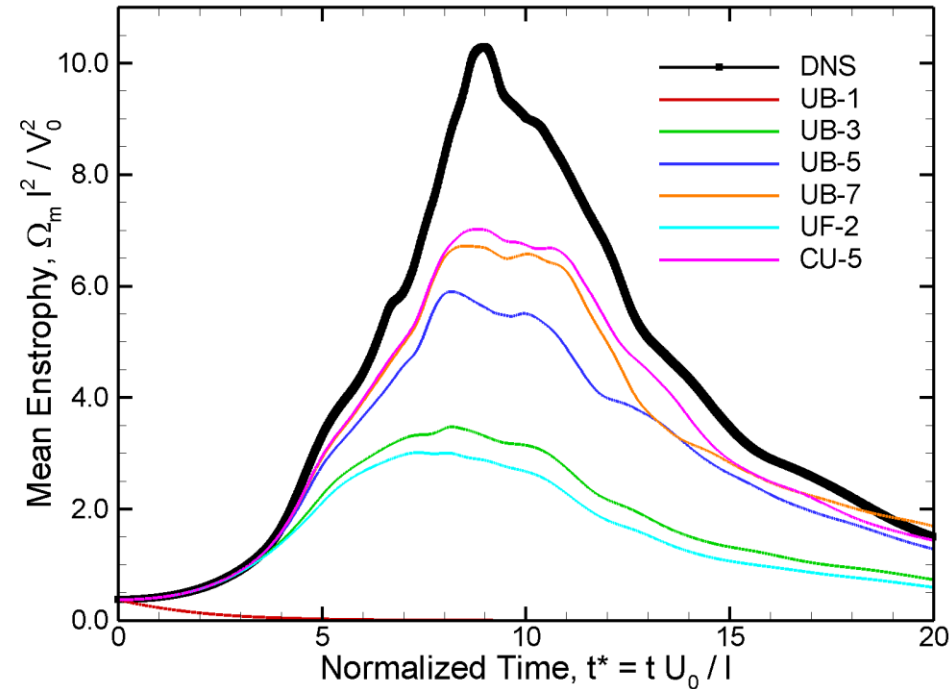


# Mean Enstrophy History 128 × 128 × 128 Point Grid

## Central Difference Schemes



## Upwind Schemes



- ◆ The central schemes generally follow the DNS enstrophy history very well, though CD-2 misses the peak at  $t^* = 9$
- ◆ The UB-1 scheme rapidly dissipates all enstrophy in the flow
- ◆ The remaining upwind schemes also all fail to match the DNS, with UF-2 having the worst agreement, and CU-5 the best



# Turbulent Channel Flow Problem

---

Air at  $P_0 = 25331$  Pa,  $T_0 = 25$  °C,  $R = 287$  J/Kg-K,  $\rho_0 = 0.296033$  Kg/m<sup>3</sup>,  
 $a_0 = 346.117$  m/s,  $u_m = 44.44$  m/s,  $\mu_0 =$  Sutherland relation,  
 $Re_{2h} = \rho_0 U_m 2h / \mu_0 = 14300$

$$u(x,y,z,t=0) = u_{c,0}[1 - (y/h)^8] + U_0 \pi \cos(2x/h) \sin(\pi y/h) \sin(2z/h),$$

$$v(x,y,z,t=0) = -U_0 \sin(2x/h) [1 + \cos(\pi y/h)] \sin(2z/h),$$

$$w(x,y,z,t=0) = -(U_0 \pi / 2) \sin(2x/h) \sin(\pi y/h) \cos(2z/h)$$

where  $0 \leq x \leq 2\pi h$ ,  $-h \leq y \leq h$ ,  $0 \leq z \leq \pi h$ ,  $h = 0.01$  m,  $u_{c,0} = 50$  m/s,  $U_0 = 5$  m/s

Grids:  $128 \times 129 \times 128$ ,  $96 \times 129 \times 96$ ,  $64 \times 129 \times 64$  and  $48 \times 129 \times 48$  grid points, uniform spacing and periodic B.Cs. in x- and z-directions, nonuniform spacing and viscous wall B.C. in y-direction

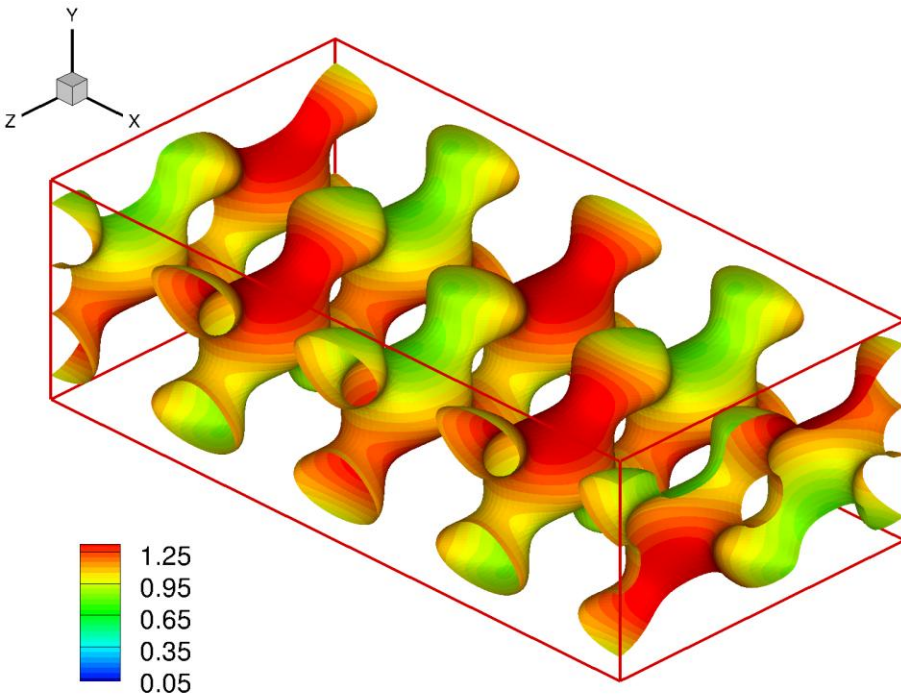
4-stage Runge-Kutta time advancement,  $CFL \approx 2.45$  based on wall-normal grid spacing at wall and acoustic wavespeed

Survey of experimental results reported by Dean (1978), and extensive DNS studies [Kim et al. (1987) and Moser et al. (1999)] have also been performed

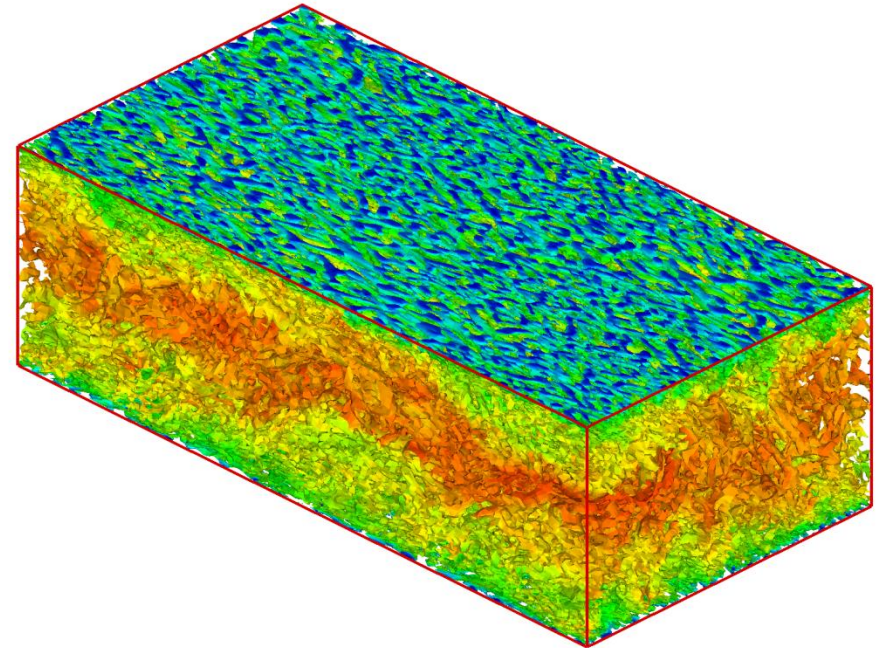


# Iso-surfaces of Q-criterion $Q = 0.1 (u_m/h)^2$

## Turbulent Channel Flow Problem at $Re_{2h} = 14300$



$t^* = 0$



$t^* = 30$

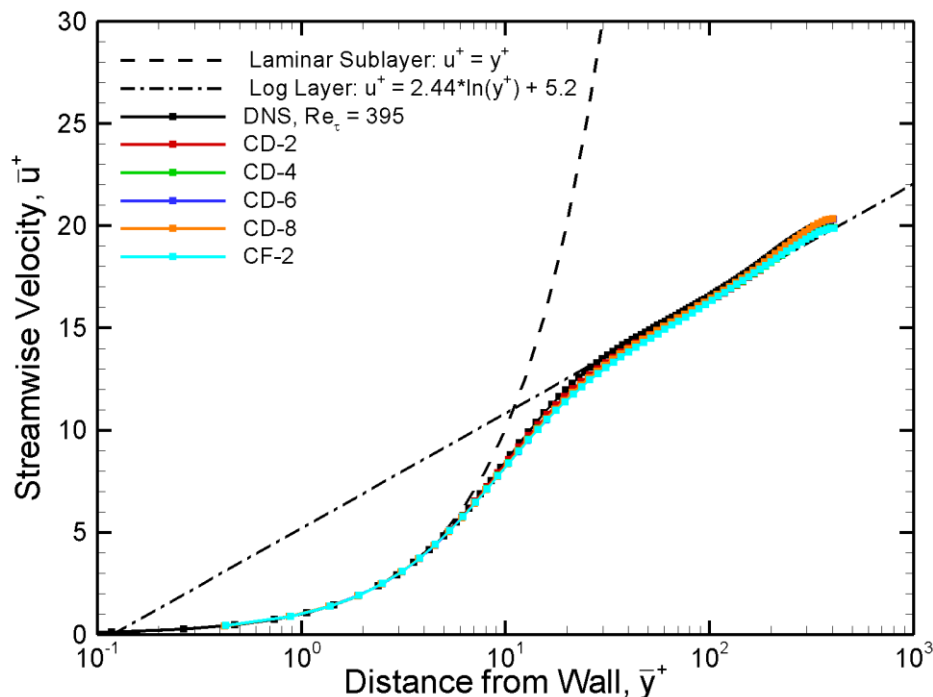
- ◆ Simulation run using CD-8 scheme on  $128 \times 129 \times 128$  point grid
- ◆ Iso-surfaces colored by velocity magnitude  $U/u_m$
- ◆  $t^*$  is a normalized timescale  $tu_m/2\pi h$



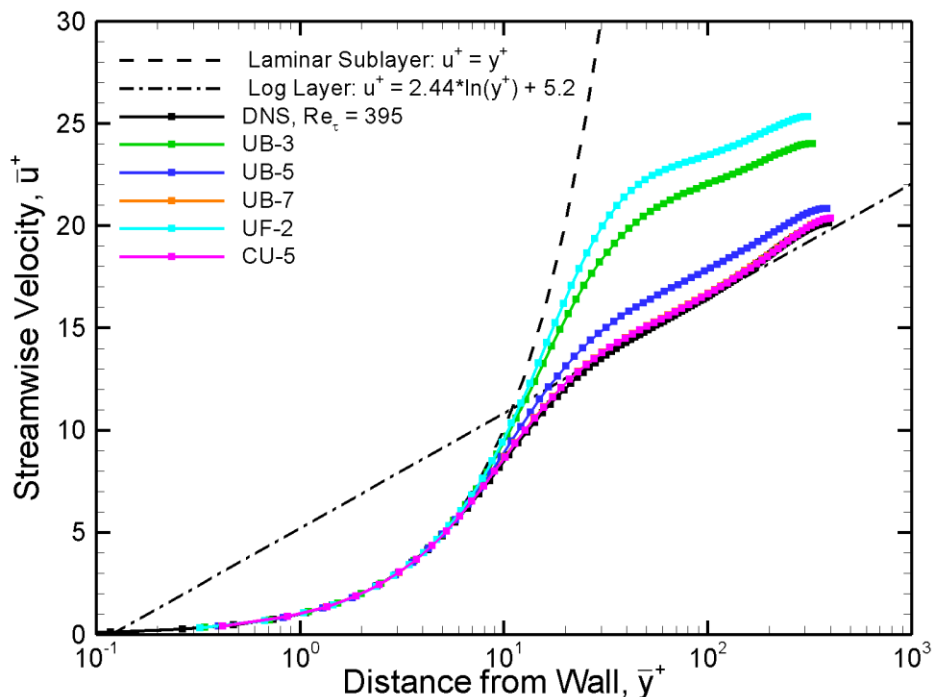
# Streamwise Velocity Profiles

## 128 × 129 × 128 Point Grid

### Central Difference Schemes



### Upwind Schemes



- ◆ Time- and space-averaged results are normalized by wall-variables
- ◆ All of the central schemes exhibit excellent agreement with the DNS, and merge smoothly from the laminar sublayer to the log layer
- ◆ The UB-1 scheme (not shown) completely laminarizes the flow
- ◆ UB-7 and CU-5 also exhibit very good agreement with the DNS
- ◆ UB-5, UB-3 and UF-2 are progressively worse, and increasingly rise above the log layer

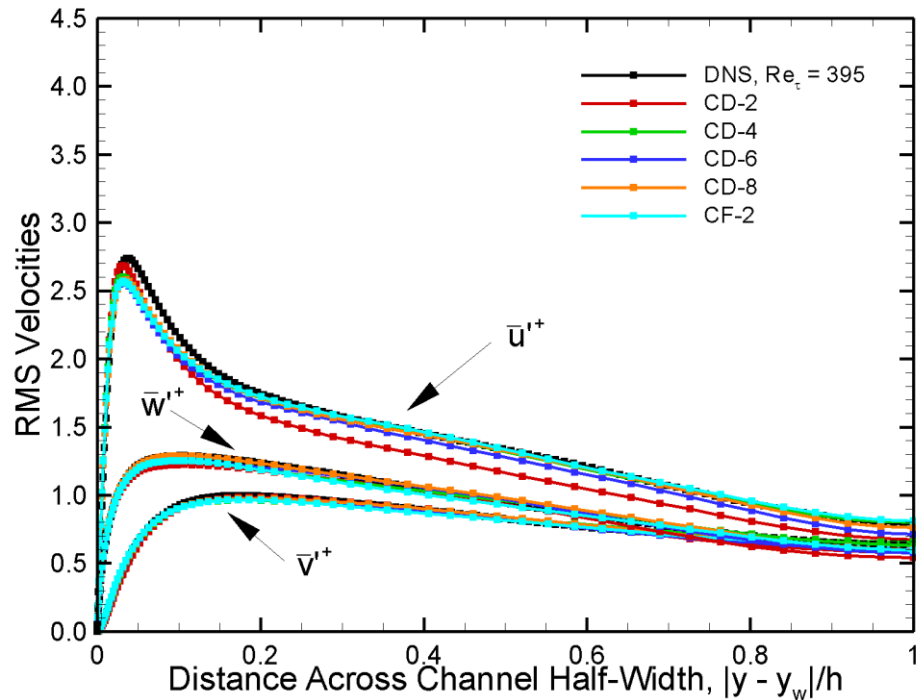




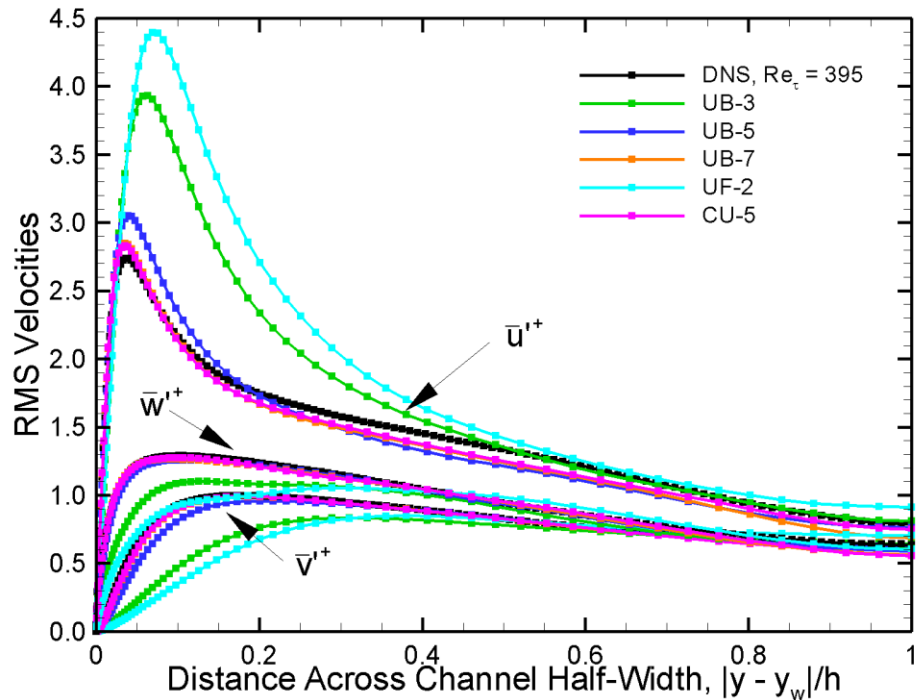
# RMS Velocity Profiles

## 128 × 129 × 128 Point Grid

### Central Difference Schemes



### Upwind Schemes



- ◆ Time- and space-averaged results are normalized by wall-variables
- ◆ The central schemes also show generally excellent agreement with the DNS RMS velocities, though CD-2 is not quite as good for  $u'^+$
- ◆ The UB-1 scheme (not shown) completely laminarizes the flow
- ◆ UB-7 and CU-5 also exhibit very good agreement with the DNS
- ◆ UB-5, UB-3 and UF-2 are progressively worse, with  $u'^+$  peaking at higher values further away from the wall, while the peaks of  $v'^+$  and  $w'^+$  decrease

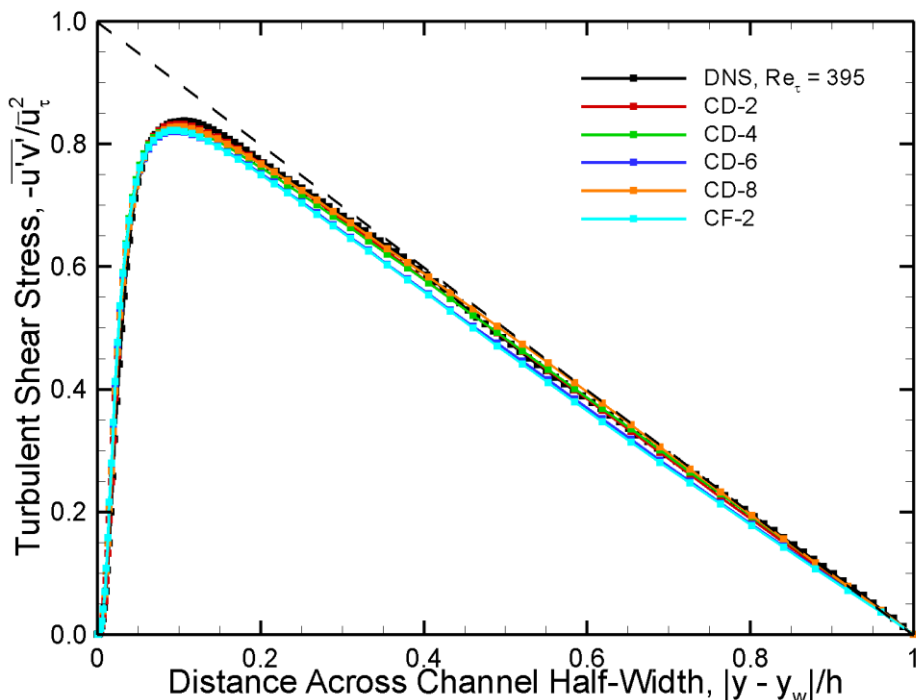




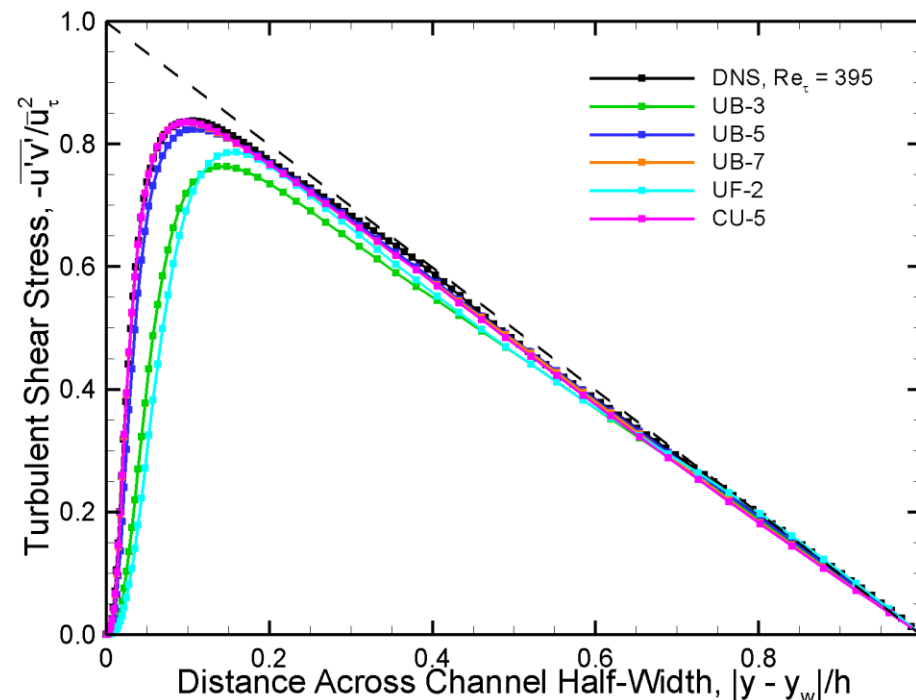
# Turbulent Shear Stress, $-u'v'/u_\tau^2$

## 128 × 129 × 128 Point Grid

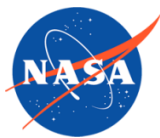
### Central Difference Schemes



### Upwind Schemes



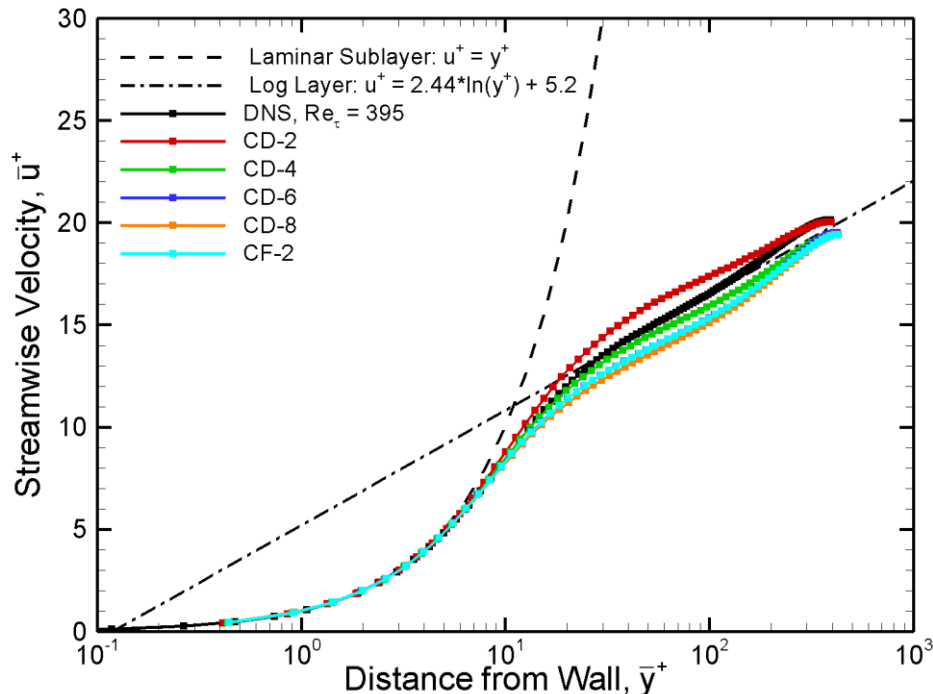
- ◆ Time- and space-averaged results are normalized by wall-variables
- ◆ All of the central schemes exhibit excellent agreement with the DNS
- ◆ The UB-1 scheme (not shown) completely laminarizes the flow
- ◆ UB-7, CU-5 and even UB-5 also exhibit very good agreement with the DNS
- ◆ UB-3 and UF-2 are progressively worse



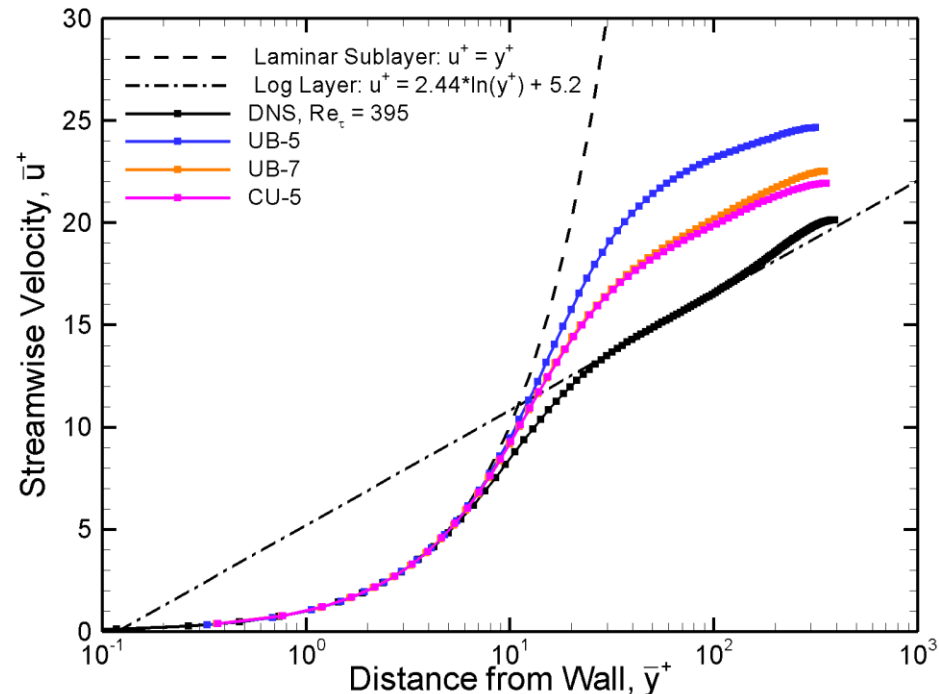
# Streamwise Velocity Profiles

## 48 × 129 × 48 Point Grid

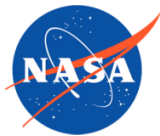
### Central Difference Schemes



### Upwind Schemes



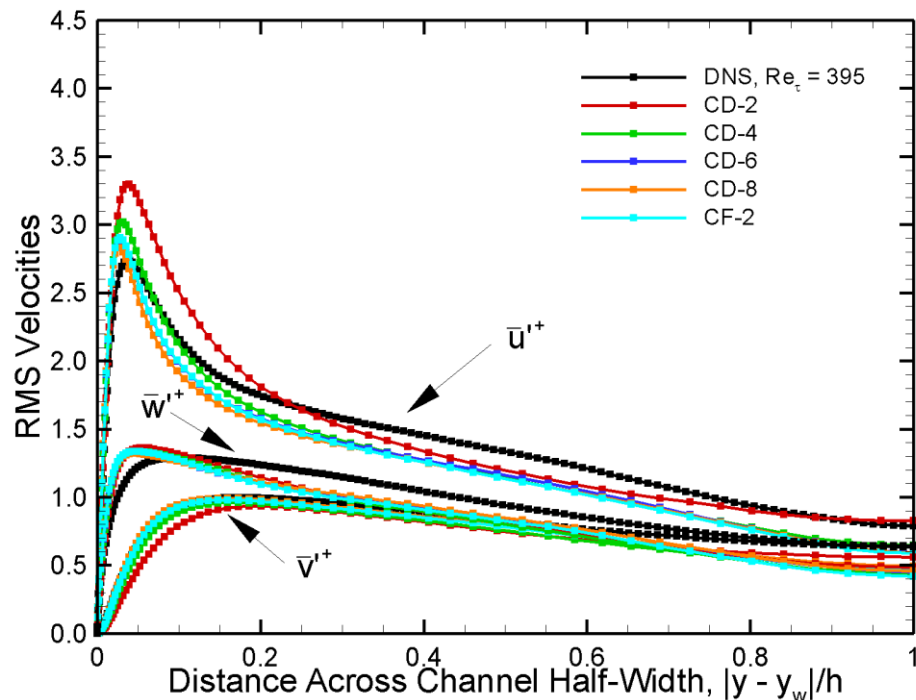
- ◆ Time- and space-averaged results are normalized by wall-variables
- ◆ CD-6, CD-8 and CF-2 are consistently offset below the log layer
- ◆ CD-4 and CD-2 are closer to the log layer but now have the wrong slope
- ◆ UB-1, UB-3 and UF-2 (not shown) completely laminarize the flow
- ◆ CU-5, UB-7 and UB-5 are progressively offset above the log layer



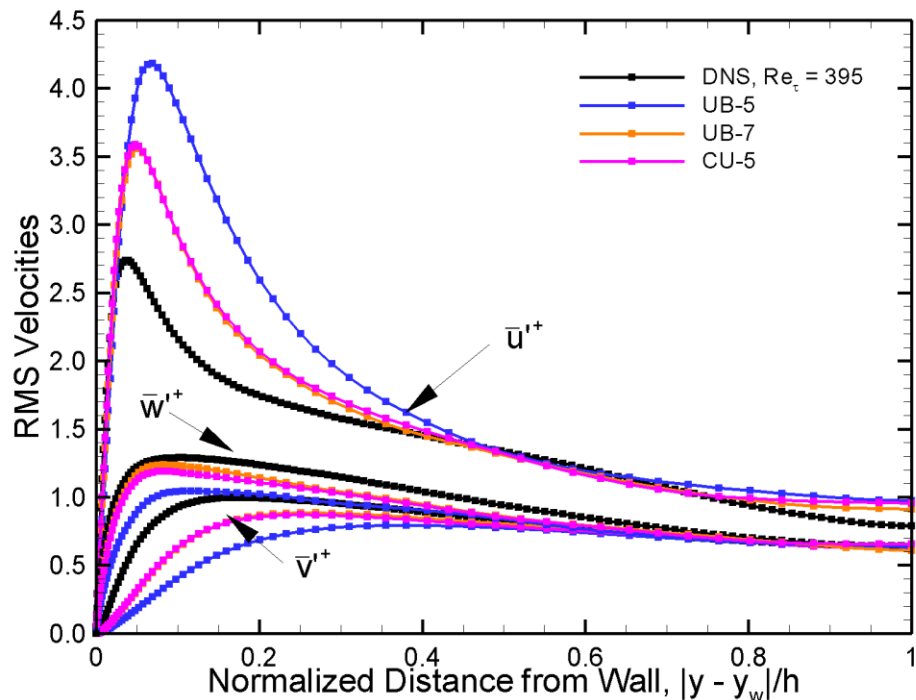
# RMS Velocity Profiles

## 48 × 129 × 48 Point Grid

### Central Difference Schemes



### Upwind Schemes



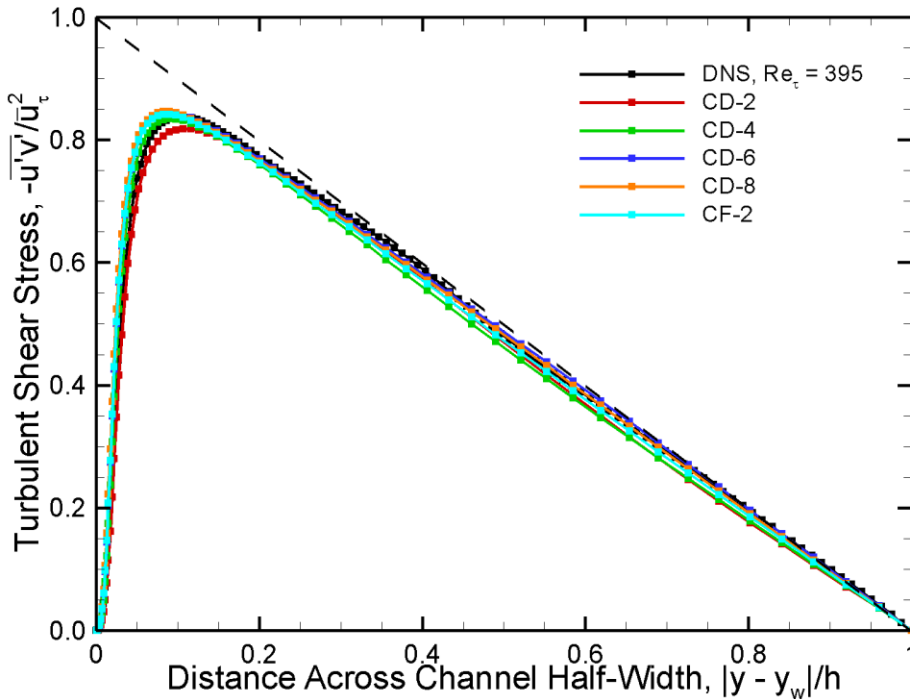
- ◆ Time- and space-averaged results are normalized by wall-variables
- ◆ None of the central difference schemes match the DNS RMS velocity profiles very well, with CD-2 having the worst agreement
- ◆ UB-1, UB-3 and UF-2 (not shown) completely laminarize the flow
- ◆ CU-5, UB-7 and UB-5 are progressively worse in predicting the DNS results, with  $u'^+$  peaking at higher values further away from the wall, while the peaks of  $v'^+$  and  $w'^+$  decrease



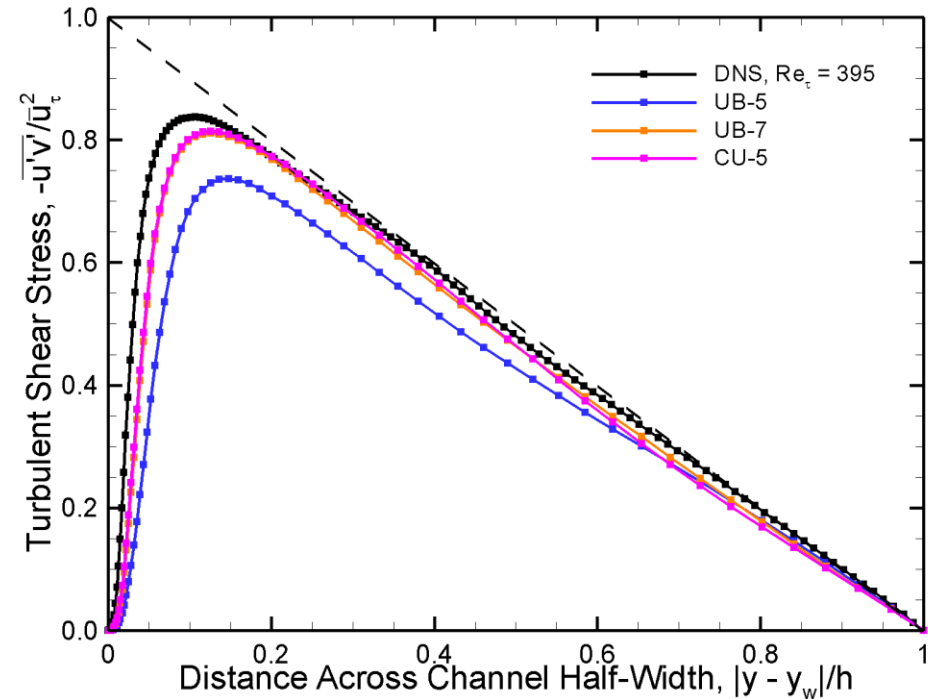
# Turbulent Shear Stress, $-u'v'/u_\tau^2$

## 48 × 129 × 48 Point Grid

### Central Difference Schemes



### Upwind Schemes

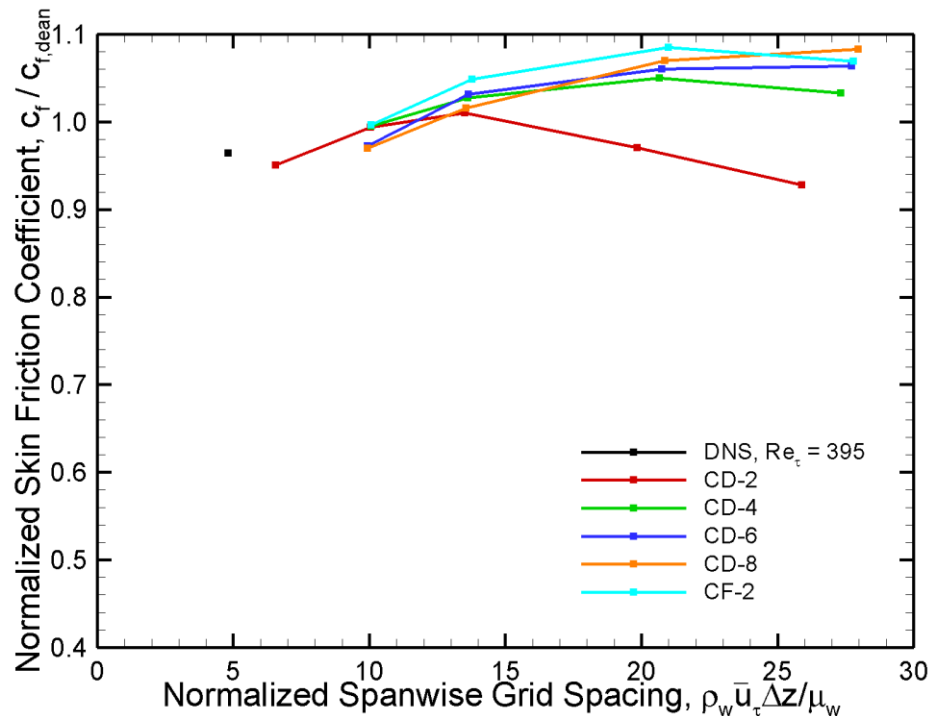


- ◆ Time- and space-averaged results are normalized by wall-variables
- ◆ All of the central schemes exhibit good agreement with the DNS, though some differences are more evident for CD-2 than the other schemes
- ◆ UB-1, UB-3 and UF-2 (not shown) completely laminarize the flow
- ◆ CU-5, UB-7 and UB-5 are in progressively worse agreement with the DNS

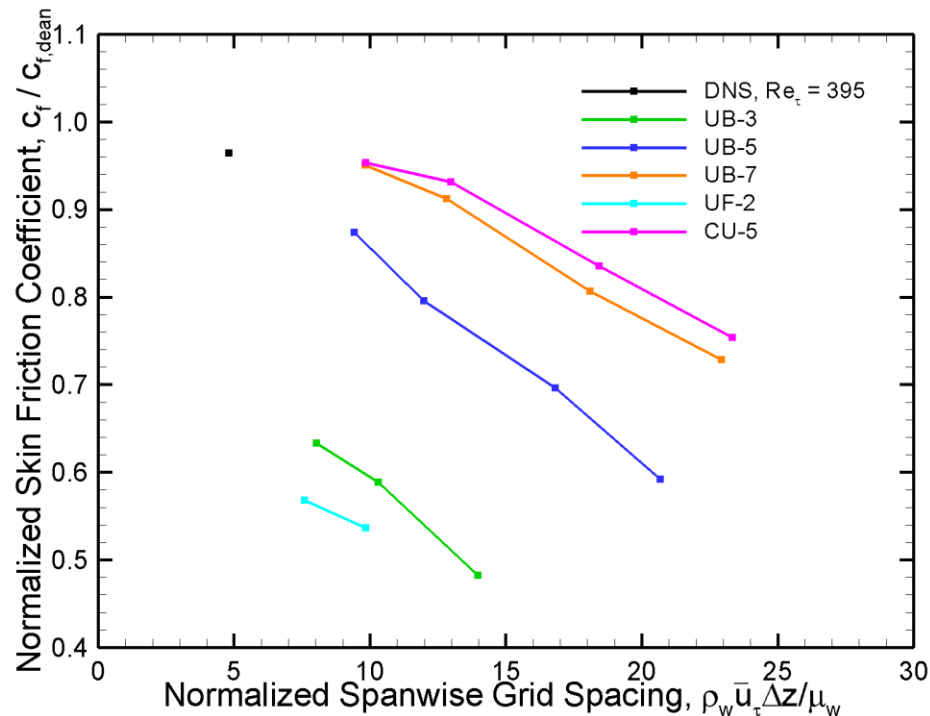


# Effect of Spanwise Grid Spacing on Average Skin Friction Coefficient, $c_f/c_{f,dean}$

## Central Difference Schemes



## Upwind Schemes



- ◆  $C_{f,dean} = 0.073 Re_{2h}^{-0.25} = 6.68 \times 10^{-3}$  for these cases
- ◆ All central schemes provide a good prediction of  $c_f$  for  $\Delta z^+ \leq 10$ , while at larger values of  $\Delta z^+$  the higher-order schemes overpredict  $c_f$ . CD-2 underpredicts  $c_f$  on the coarsest grids.
- ◆ CU-5 and UB-7 yield an excellent prediction of  $c_f$  for  $\Delta z^+ \leq 10$ , and a reasonable prediction (within 10%) for for  $\Delta z^+ \leq 13$ . UB-5 may be good for for  $\Delta z^+ \approx 5$ . UB-3 and UF-2 are very poor in predictive accuracy.



# Summary

---

- ◆ **Five different central difference schemes, based on a conservative differencing form of the Kennedy and Gruber skew-symmetric scheme, were compared with six different upwind schemes based on primitive variable reconstruction and the Roe flux**
- ◆ **These eleven schemes were tested on a one-dimensional acoustic standing wave problem, the Taylor-Green vortex problem and a turbulent channel flow problem**
- ◆ **The central schemes were generally very accurate and stable, provided the grid stretching rate was kept below 10%. As near-DNS grid resolutions, the results were comparable to reference DNS calculations. At coarser grid resolutions, the need for an LES SGS model became apparent. There was a noticeable improvement moving from CD-2 to CD-4, and higher-order schemes appear to yield clear benefits on coarser grids**
- ◆ **The UB-7 and CU-5 upwind schemes also performed very well at near-DNS grid resolutions. The UB-5 upwind scheme does not do as well, but does appear to be suitable for well-resolved DNS. The UF-2 and UB-3 upwind schemes, which have significant dissipation over a wide spectral range, appear to be poorly suited for DNS or LES.**